

Continuous Self Energy of Ions at the Dielectric Interface

Rui Wang¹ and Zhen-Gang Wang^{1,*}

¹*Division of Chemistry and Chemical Engineering,
California Institute of Technology, Pasadena, CA 91125, USA*

We present a simple, unified theory for the self-energy of an ion near a dielectric interface. Our theory accounts for both the short-range (solvation) and long-range (image force) electrostatic forces, charge polarization induced by these forces, and the cavity energy. In contrast to previous models, our self energy is continuous across the interface and thus applicable to both the water and air (oil) sides of the interface. With no fitting parameters, we predict the specific ion effect on the interfacial affinity of halogen anions at the water/air interface, and the strong adsorption of hydrophobic ions at the water/oil interface, in agreement with experiments and atomistic simulations.

PACS numbers: 82.45.Gj, 61.20.Qg, 05.20.-y, 68.03.Cd

The interfacial activities of salt ions are of great importance in physical chemistry, colloidal science and biophysics[1]. Many interfacial phenomena, such as the surface tension of electrolyte solution[2], salt effects on bubble coalescence[3] and effectiveness of salts on the stability of proteins solutions and colloidal suspensions[4], exhibit strong dependence on the chemical identity of the ions. Although this “specific ion effect” has been known for over a century[5], a systematic, unified and predictive theoretical framework that is able to capture all the essential physics of the specific ion effect remains an outstanding challenge. Current theoretical descriptions are system dependent and require adjustable parameters to force-fit experimental data[6]. For example, a common practice is to invoke ad hoc short-range potentials for the different ions[7, 8] or artificially restrict the ions to different locations with respect of the interface[9].

A key factor that determines the ion distribution at the dielectric interface as well as other interfacial properties is the self energy of a single ion[10]. Theoretical efforts to account for the effect of self energy near an interface were pioneered by Wagner, Onsager and Samaras (WOS)[11]. The WOS theory predicts depletion of ions from the water/air interface due to the image charge repulsion – part of the self energy – and qualitatively explains the increase of surface tension with the salt concentration at the water/air interface. However, this theory fails to capture the initial decrease with salt concentration in the tension at water/air (oil) interfaces known as the Jones-Ray effect[12], and the systematic dependence on the identity of the ions known as the Hofmeister series effect[2].

A major weakness in the WOS theory and its subsequent modifications is modeling the ion as a point charge, which results in a discontinuous self energy across the dielectric interface. The self energy diverges to positive infinity when an ion approaches the interface from the water side, making the ion concentration zero at the interface and by extension in the entire zone on the other side of the interface. The picture of an ion-free zone in the WOS theory contradicts data from both experiments[13] and simulation[14] which show ions are able to penetrate

to the air-side of the Gibbs dividing surface and can even be adsorbed to it. On the other hand, when an ion approaches the interface from the air(oil) side, the point charge model predicts a diverging self energy to negative infinity, which would imply unlimited accumulation of ions there. To avoid this unrealistic behavior, the ion distribution is artificially restricted to lie only in the water phase, which precludes the application of the theory from describing hydrophobic ions and liquid-liquid interfaces. This artificial cut-off also affects the gradient of the electrostatic potential across the interface, which is shown essential to the initial drop of the surface tension in the Jones-Ray effect[15].

Another important effect missing in the point charge model in the WOS theory as well as the conductor ion model of Ulstrup and Kharkats[16] is the finite polarizability of the ions. Polarizability is an intrinsic property of specific ions, and can vary substantially between different ions. Computer simulation by Jungwirth and Tobias[14] showed that the polarizability of ions is a key contribution to their differential affinity to the interface. Recently, Levin and coworkers [17, 18] developed a model for the self energy of polarizable ions near a dielectric interface to explain several interfacial properties of electrolyte solutions. In their model, charge polarization in the ion is included to optimize the short-range Born solvation energy. However, near a dielectric interface, the long-range image force, which can either enhance or counteract the Born solvation energy, is strong enough to contribute to charge polarization in the ion. The imposition of a cut-off in the ion distribution in their work also makes it difficult to extend the theory to hydrophobic ions and to liquid-liquid interfaces.

In this Letter, we present a unified theory for the self energy of an ion near a dielectric interface that includes all the essential components: the Born solvation energy, the image charge interaction, ion polarizability and cavity energy. Our theory yields a continuous self energy across the interface, thus resolving the divergence problems in previous models and allowing a unified description of the ions on both sides of the interface. All the

electrostatic contributions are treated in a single, consistent framework. In particular, the polarization of the ion has a significant contribution from the image charge interaction. Within the framework of a sharp-interface, dielectric model for the solvents, our theory is free from adjustable parameters and requires no artificial imposition of cut-off. Using the intrinsic parameters of the ion, such as the valency, radius, polarizability, and of the solvent (reflected in the hydrophobicity cavity parameter, which can be estimated independently), we are able to predict a wide range of specific ion effects, such as the Hofmeister series effect of the interfacial affinity of halogen anions at the water/air interface and the strong adsorption of hydrophobic ions at the oil side of the water/oil interface.

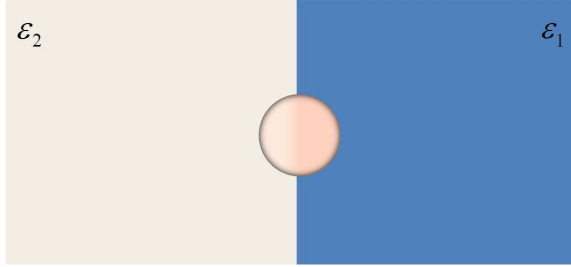


FIG. 1: Schematic description of the model system. The charge distribution on the ion is illustrated by the shade.

As illustrated in Fig. 1, we consider a single ion in the vicinity of a sharp interface between two semi-infinite regions (\mathcal{R}_1 and \mathcal{R}_2) with respective dielectric constant ε_1 and ε_2 ($\varepsilon_1 > \varepsilon_2$). We choose our coordinate system such that the interface is located at $z = 0$. The elementary charge e is taken as the unit of charge, and kT is used as the unit of energy. The ion is taken to be a spherical particle of radius a centered at \mathbf{r}_c , with a short-range charge distribution function $\rho(\mathbf{r}, \mathbf{r}_c)$, which satisfies $\int d\mathbf{r} \rho(\mathbf{r}, \mathbf{r}_c) = \nu_{\pm}$ with ν_{\pm} the valency of the ion (“+” for cation and “−” for anion). The ion is polarizable; therefore, the charge distribution will be self-adjusted to the local dielectric environment. The total self energy of the ion can be divided into three parts:

$$u(\mathbf{r}_c) = u_{ele}(\mathbf{r}_c) + u_{pol}(\mathbf{r}_c) + u_{cav}(\mathbf{r}_c) \quad (1)$$

where u_{ele} , u_{pol} and u_{cav} are contributions from the electrostatic interaction, the energy cost of polarization and the cavity energy, respectively. u_{ele} accounts for the sum of the electrostatic interactions in the constituent charges on the ion:

$$u_{ele}(\mathbf{r}_c) = 2\pi l_B \int d\mathbf{r} \int d\mathbf{r}' \rho(\mathbf{r}, \mathbf{r}_c) G(\mathbf{r}, \mathbf{r}') \rho(\mathbf{r}', \mathbf{r}_c) \quad (2)$$

where $l_B = e^2/4\pi\varepsilon_0 kT$ is the Bjerrum length in the vacuum and ε_0 is the vacuum permittivity. $G(\mathbf{r}, \mathbf{r}')$ is the Green’s function, i.e., the electrostatic potential at \mathbf{r} due to a unit point charge at \mathbf{r}' . It satisfies the Poisson equation $-\nabla \cdot [\varepsilon(\mathbf{r}) \nabla G(\mathbf{r}, \mathbf{r}')] = \delta(\mathbf{r} - \mathbf{r}')$. Depending on

whether \mathbf{r} and \mathbf{r}' are in the same region, $G(\mathbf{r}, \mathbf{r}')$ is given by

$$G(\mathbf{r}, \mathbf{r}') = \begin{cases} \frac{1}{\varepsilon_{\alpha} |\mathbf{r} - \mathbf{r}'|} + \frac{\Delta_{\alpha\beta}}{\varepsilon_{\alpha} |\mathbf{r} - \mathbf{r}^*|} & \mathbf{r}, \mathbf{r}' \in \mathcal{R}_{\alpha} \\ \frac{2}{(\varepsilon_{\alpha} + \varepsilon_{\beta}) |\mathbf{r} - \mathbf{r}'|} & \mathbf{r} \in \mathcal{R}_{\beta}, \mathbf{r}' \in \mathcal{R}_{\alpha} \end{cases} \quad (3)$$

α and β can be either 1 or 2, and $\Delta_{\alpha\beta} = (\varepsilon_{\alpha} - \varepsilon_{\beta})/(\varepsilon_{\alpha} + \varepsilon_{\beta})$ is the dielectric contrast. $\mathbf{r}^* = (x', y', -z')$ is the location of the image of \mathbf{r}' with respect to the plane of the interface. The first term on the r.h.s of Eq. 3 is the direct Coulomb interaction and will generate the local Born solvation energy upon integration over the charge distribution. The last term in the first line of Eq. 3 describes the distortion of electrostatic potential due to the dielectric discontinuity, manifested as an image charge interaction. This term can be either positive or negative depending on whether the point charge is located on the high dielectric side or low dielectric side; thus it either enhances or counteracts the solvation energy effect. Both the local and long-range electrostatic effects are included by Eqs. 2 and 3.

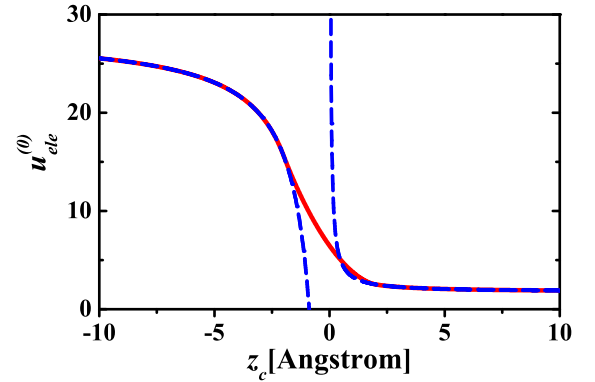


FIG. 2: Electrostatic part of the self energy, u_{ele} , of a monovalent ion with uniform surface charge distribution, calculated by our model (solid line) and the point charge model adjusted by the bulk Born energy (dash line). $\varepsilon_1 = 80$, $\varepsilon_2 = 5$ and $a = 2\text{\AA}$.

In the point charge model $\rho(\mathbf{r}, \mathbf{r}_c) = \nu_{\pm} \delta(\mathbf{r} - \mathbf{r}_c)$, Eq. 2 gives $u_{ele}(\mathbf{r}_c) = 2\pi l_B \nu_{\pm}^2 G(\mathbf{r}_c, \mathbf{r}_c)$, which produces divergences in both the local Born solvation energy and in the image charge interaction as $z_c \rightarrow 0$ from either side of the interface. The use of a finite charge distribution avoids both types of divergences. Fig. 2 shows the result for the electrostatic part of the self energy, $u_{ele}^{(0)}$, calculated for a fixed, uniform surface charge distribution on the ion (the superscript (0) denotes fixed charge distribution, i.e., a nonpolarizable ion). For comparison, we include the results from the point-charge model, adjusted by the bulk Born energy $\nu_{\pm}^2 l_B / 2a\varepsilon_{\alpha}$ on each side. While $u_{ele}^{(0)}$ calculated by the two models are consistent in the bulk region ($|z_c| > a$), qualitative and dramatic differences are seen in the interfacial region – the most relevant region for

the interfacial activities of the ions. Interestingly, $u_{ele}^{(0)}$ for an ion located exactly at the interface ($z_c = 0$) is significantly lower than the algebraic mean of the Born solvation energy in two bulk regions.

Polarization of the ion allows the charge distribution to self-adjust to its local dielectric environment, which decreases u_{ele} relative to that for a fixed uniform surface charge distribution. This redistribution incurs an energy penalty u_{pol} . Following the idea proposed by Levin [17], we take u_{pol} to be:

$$u_{pol}(\mathbf{r}_c) = \frac{(\gamma_0 - \gamma)}{v\gamma} \int d\mathbf{r} \left[\frac{\rho(\mathbf{r}, \mathbf{r}_c)}{\rho_0} - 1 \right]^2 \quad (4)$$

where γ is the polarizability of the ion, $\gamma_0 (= a^3)$ is the polarizability of a perfectly polarizable ion of the same radius, v is the volume of the ion, and ρ_0 is the charge density for the uniform spherical distribution. The ion with larger γ can more easily adjust its charge distribution to reduce the electrostatic energy.

Finally, u_{cav} in Eq. 1 is the work required to create a cavity for the ion where the liquid molecules are excluded. For aqueous solvent, this cavity energy arises primarily due to the disruption of the hydrogen bond network. For the water/air (oil) interface (we assume water to be on the $z > 0$ side), u_{cav} is given by [17, 21]

$$u_{cav}(\mathbf{r}_c) = \begin{cases} \kappa a^3 & \text{for } z_c \geq a \\ \frac{\kappa a^3}{4} \left(\frac{z_c}{a} + 1 \right)^2 (2 - \frac{z_c}{a}) & \text{for } a > z_c \geq -a \\ 0 & \text{for } z_c < -a \end{cases} \quad (5)$$

with $\kappa \approx 0.3 \text{ \AA}^{-3}$ from bulk simulation [22]. u_{cav} provides the driving force for the ion to migrate from the bulk water towards the interface; this driving force is larger for larger ions.

Putting together Eqs. 2, 4 and 5, we obtain the general expression for the self energy of an ion with arbitrary charge distribution on the ion. The optimal distribution is then obtained from $\delta u(\mathbf{r}_c)/\delta \rho(\mathbf{r}, \mathbf{r}_c) = 0$. To avoid the complexity of solving the high dimensional integral equation from this condition, we construct a variational trial function for $\rho(\mathbf{r}, \mathbf{r}_c)$. We assume that polarization apportions respectively f and $1 - f$ of the total ionic charge ($f \in [0, 1]$) uniformly to the two hemispheres of the ion separated by the xy plane at z_c . Thus, $\rho(\mathbf{r}, \mathbf{r}_c)$ takes the following form

$$\rho(\mathbf{r}, \mathbf{r}_c) = \begin{cases} 2f\rho_0(\mathbf{r}) & \text{for } z \geq z_c \\ 2(1-f)\rho_0(\mathbf{r}) & \text{for } z < z_c \end{cases} \quad (6)$$

where $\rho_0(\mathbf{r}) = \nu_{\pm} \delta(|\mathbf{r} - \mathbf{r}_c| - a)/4\pi a^2$ is the uniform surface distribution on the sphere. The deviation of f from 1/2 measures the degree of polarization of the ionic charge. Substituting the trial function Eq. 6 into Eqs. 1, 2 and 4, $u(\mathbf{r}_c)$ can be simplified to a quadratic function

of f , which can be easily minimized to yield a position-dependent charge fraction $f(\mathbf{r}_c)$. This optimal charge fraction $f(\mathbf{r}_c)$ is then used to evaluate $u(\mathbf{r}_c)$. Since the electrostatic interaction includes the local Born solvation energy and the long-range image charge force, the resulting polarization reflects the combined effects of these terms.

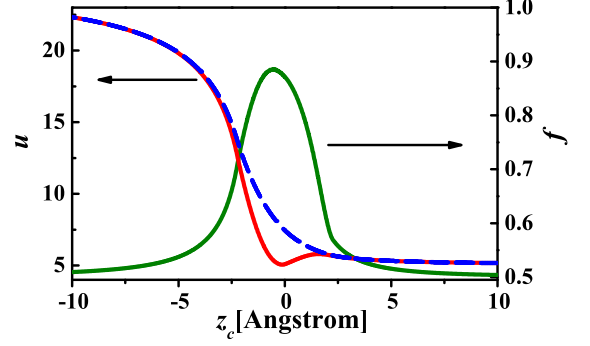


FIG. 3: Polarization effect on the self energy of I^- : the fraction of ionic charge on the hemisphere faced to the high dielectric side ($z > z_c$) and the self energy of I^- (solid line) in comparison with the nonpolarizable ion of the same radius as I^- (dash line). $\epsilon_1 = 80$, $\epsilon_2 = 5$.

Fig. 3 shows the charge polarization and self energy for I^- ($a_{\text{I}^-} = 2.26 \text{ \AA}$, $\gamma_{\text{I}^-} = 6.9 \text{ \AA}^3$). In the immediate vicinity of the interface ($|z_c| < a$), I^- is highly polarized: over 80% of the ionic charge resides on the hemisphere facing the high dielectric side ($z > z_c$). The charge relocation reduces the exposure of charge to the low dielectric environment, which tempers the increase of the electrostatic self energy as the ion penetrates to the interface from the high dielectric side. On the other hand, the cavity energy is decreased by releasing the space for the recovery of the hydrogen bond network. The decrease in cavity energy at the relatively low cost of electrostatic self energy leads to a local minimum at the interface in the self energy profile. In contrast, the self energy of a nonpolarizable ion with the same radius as I^- increases monotonically. This indicates that charge polarization is essential to making it energetically favorable for the I^- ion to migrate towards the interface. Beyond the immediate vicinity of the interface ($|z_c| > a$), polarization is driven by the long-range image charge effect, and f decays to 1/2 as the ion approaches the bulk. While the effect of charge polarization on the self energy is small on the high dielectric side beyond $z_c = a$, the self energy of the polarizable ion is appreciably lower than the nonpolarizable ion on the low dielectric side slightly beyond $z_c = -a$, as a result of stronger and longer-range image force in this region. The feature of a local minimum in the self energy profile of I^- at the interface obtained by our theory is consistent with the result of MD simulation that used a polarizable potential model [19].

The self energy profile of the ion across the interface is determined by the competition between the cavity energy and the electrostatic contribution, the former preferring for the ion to reside on the air (oil) side and the latter favoring it being on the aqueous side. The cavity energy is only related to the ion size, while the electrostatic self energy depends on both the ion size and the charge polarization. Figure 4(a) shows u for four halogen anions and the alkali-metal Na^+ . We use the Born radius 2.26, 2.05, 1.91, 1.46 and 1.80 Å[20], and the polarizability 6.90, 4.53, 3.50, 0.97 and 0.18 Å³[14], respectively for I^- , Br^- , Cl^- , F^- and Na^+ . For the larger and more polarizable ions, such as I^- and Br^- , the gain in the cavity energy is significant as the ion moves into the interfacial region from the aqueous bulk. On the other hand, the cost of the electrostatic self energy is substantially reduced due to the charge polarization. The combination of these two effects leads to a local minimum of u at the interface. In contrast, u is monotonic for small and less polarizable ions, such as F^- and Na^+ , because the gain in the cavity energy cannot offset the rapid increase of the electrostatic self energy on migration from the aqueous phase to the air (oil) phase. For the intermediate case Cl^- , these two energies balance each other, giving rise to a plateau in the u profile.

The self energy of an ion is closely related to the concentration profile of the ions. While a full treatment has to account for the charge neutrality and interaction between the ions, which will give rise to screening of the long-range image forces, we can obtain a qualitative picture of the ion distribution by defining the interfacial affinity as $e^{-[u(z_c)-u(\infty)]}$ to characterize the relative probability of finding the ion in the interfacial region to the bulk. In Fig. 4(b), we show the interfacial affinity for the halogen anions and Na^+ . It is clear that our theory captures the known specific ion effect, which follows precisely the reverse Hofmeister series: $\text{I}^- > \text{Br}^- > \text{Cl}^- > \text{F}^-$ [2, 5]. The local peak in the interfacial affinity of I^- and Br^- ions is consistent with results of electron spectroscopy experiments [13] and computer simulations using polarizable fields [14]. In addition, we see that the interfacial affinity of halogen anions are larger than that of Na^+ , from which we expect local charge separation and an induced electrical double layer at the interface in a NaX solution ($\text{X}=\text{I}, \text{Br}, \text{Cl}, \text{F}$), with the halogen anions accumulating right around the location of the interface and the Na^+ ions next to it on the water side. The electrical double layer generates an electric field pointing from the water side to the air (oil) side. From Fig. 4(b), we expect the degree of charge separation and the strength of the electric field to be stronger for solutions of NaI and NaBr than NaF . The existence of electrostatic potential difference between a bulk electrolyte solution and the interface has been a long-standing puzzle in physical chemistry[23]. The difference in the self energy between the cations and anions offers a natural explanation of this phenomenon.

The continuous nature of the self energy across the interface allows more accurate calculation of the electrostatic potential gradient, which has been shown to be key to explaining the Jones-Ray effect[15].

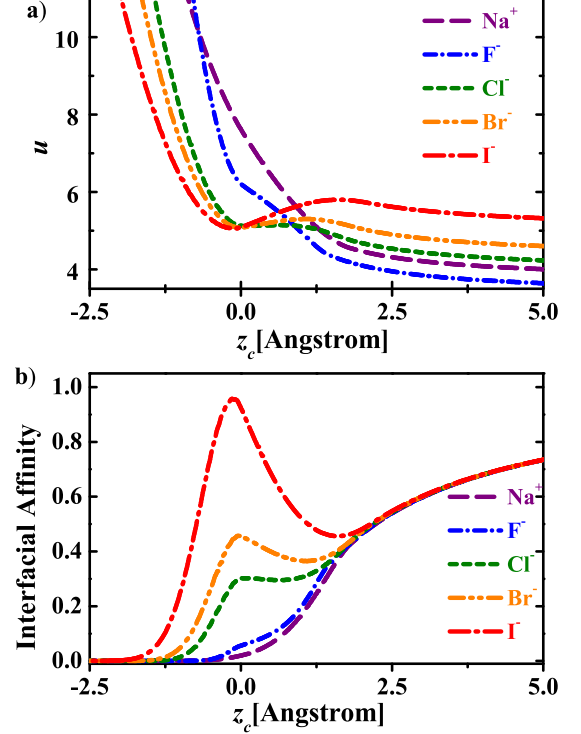


FIG. 4: (a) Self energy and (b) interfacial affinity of F^- , Cl^- , Br^- , I^- and Na^+ . $\epsilon_1 = 80$, $\epsilon_2 = 5$.

Finally, with the advantage of a continuous self energy, our theory is able to describe the hydrophobic ions that have often been excluded in existing theories[11, 17, 18]. Recently, Schlossman and coworkers observed strong adsorption of hydrophobic ions at the water/oil interface by X-ray reflectivity study[8]. The experimental data was explained by assigning some phenomenological non-monotonic one-body potentials to different ions. Within our theory, this phenomenon can be easily understood as arising from the long-range image charge attraction of the hydrophobic ions in the low-dielectric oil phase. Fig. 5 shows the interfacial affinity of the hydrophobic ion calculated by our theory. As the ion approaches the interface from the oil side, the interfacial affinity increases because of the image charge attraction, and then decreases rapidly due to the unfavorable contact with the aqueous environment (the cost of cavity energy). The factor of about two hundred in the interfacial activity on the oil side of the interface corresponds to minimum in the self energy with depth of about $5kT$. The magnitude of the interfacial activity predicted by our theory is in good agreement with the experimental results[8].

In conclusion, we have presented a new theory for the

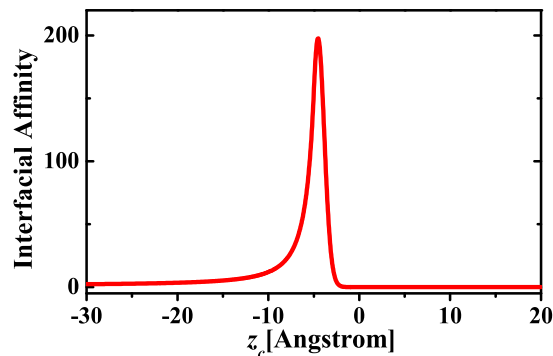


FIG. 5: Interfacial affinity of a hydrophobic ion at the water-oil interface relative to the bulk oil phase. $a = 5\text{\AA}$, $\gamma = 10\text{\AA}^3$, $\epsilon_1 = 80$ and $\epsilon_2 = 5$.

self energy of the ions which represents significant improvement over existing theories in several important respects. First, by using a finite charge distribution for the ion, our theory naturally includes the Born solvation effects and the long-range image charge effects, and resolves the divergence problem of the self energy near the interface due to the image charge, yielding a continuous self energy across the interface. Thus our theory avoids the introduction of an artificial cut-off as required in most current theoretical treatments. This feature facilitates the calculation of the electrostatic potential gradient across the electrolyte solution interface, which holds the key to explaining the Jones-Ray effect. The continuous self energy also allows treatment of both hydrophilic and hydrophobic ions within the same theoretical framework. Second, the electrostatic and polarization effects are treated in a unified and consistent manner, where both the short-range and long-range electrostatic interactions are optimized by the charge polarization. Lastly, our theory is free of fitting parameters: the interfacial properties of the ions are determined by the intrinsic parameters, such as the valency, radius and polarizability of the ions and the dielectric properties of the coexistent phases. Although a full theory is yet to be constructed for the explicit calculation of the interfacial tension and ion profiles, the behavior of the self energy can already explain/predict several qualitative phenomena: the reverse Hofmeister sequence: $\text{I}^- > \text{Br}^- > \text{Cl}^- > \text{F}^-$ in the interfacial activity; local accumulation of large halogen ions, such as I^- and Br^- ; charge separation between the cations and anions at the interface; and strong adsorption of hydrophobic ions to the oil side of the interface.

The self energy model developed here provides the essential ingredient in a complete theory to treat ions at finite concentration, via e.g., the weak coupling theory[24] or modified Poisson-Boltzmann theory[10, 25], to finally resolve the long-standing puzzles mentioned in the beginning of this Letter.

Acknowledgment is made to the Donors of the Ameri-

can Chemical Society Petroleum Research Fund for partial support of this research.

* Electronic address: zgw@caltech.edu

- [1] J. N. Israelachvili, *Intermolecular and surface forces*, Academic, 1992.
- [2] W. Kunz, P. Lo Nostro, and B.W. Ninham, *Curr. Opin. Colloid Interf. Sci.* **9**, 1 (2004); B. C. Garrett, *Science* **303**, 1146 (2004).
- [3] V. S. J. Craig, B. W. Ninham and R. M. Pashley, *Nature* **364**, 317 (1993).
- [4] Tavares, F. W., Bratko, D., Prausnitz, J. M. *Curr. Opin. Colloid Interface Sci.* **9**, 81 (2004); Gradzielski, M. *Curr. Opin. Colloid Interface Sci.* **9**, 256 (2004).
- [5] F. Hofmeister, *Arch. Exp. Pathol. Pharmacol.* **24**, 247 (1888).
- [6] P. L. Nostro and B. W. Ninham, *Chem. Rev.* **112**, 2286 (2012).
- [7] M. Boström, D. R. M. Williams and B. W. Ninham, *Langmuir* **17**, 4475 (2001); M. Manciu and E. Ruckenstein, *Adv. Colloid Interface Sci.* **105**, 63 (2003).
- [8] N. Laanait, et. al, *Proc. Natl. Acad. Sci. U.S.A.* **109**, 20326 (2012); N. Laanait, et. al, *J. Chem. Phys.* **132**, 171101 (2010); G. M. Luo et. al, *Science* **311**, 216 (2006).
- [9] M. Bier, J. Zwanikken and R. van Roij, *Phys. Rev. Lett.* **101**, 046104 (2008); D. S. Dean and R. R. Horgan, *Phys. Rev. E* **69**, 061603 (2004).
- [10] Z.-G. Wang, *Phys. Rev. E* **81**, 021501 (2010).
- [11] C. Wagner, *Phys. Z.* **25**, 474 (1924); L. Onsager and N. T. Samaras, *J. Chem. Phys.* **2**, 528 (1934).
- [12] G. Jones and W. A. Ray, *J. Am. Chem. Soc.* **59**, 187 (1937); P. B. Petersen and R. J. Saykally, *J. Am. Chem. Soc.* **127**, 15446 (2005).
- [13] S. Ghosal et al., *Science* **307**, 563 (2005).
- [14] P. Jungwirth and D. J. Tobias, *J. Phys. Chem. B* **106**, 6361 (2002); P. Jungwirth and D. J. Tobias, *Chem. Rev.* **106**, 1256 (2006).
- [15] A. Onuki, *J. Chem. Phys.* **128**, art. no. 224704 (2008); R. Wang and Z.-G. Wang, *J. Chem. Phys.* **135**, 014707 (2011).
- [16] J. Ulstrup and Y. Kharkats, *Russ. J. Electrochem.* **29**, 299 (1993).
- [17] Y. Levin, *Phys. Rev. Lett.* **102**, 147803 (2009).
- [18] Y. Levin, A. P. dos Santos and A. Diehl, *Phys. Rev. Lett.* **103**, 257802 (2009); *Langmuir*, **26**, 10778 (2010).
- [19] L. X. Dang and T.-M. Chang, *J. Phys. Chem. B* **106**, 235 (2002); T.-M. Chang and L. X. Dang, *Chem. Rev.* **106**, 1305 (2006).
- [20] W. M. Latimer, K. S. Pitzer and C. M. Slansky, *J. Chem. Phys.* **7**, 108 (1939).
- [21] K. Lum, D. Chandler, and J. D. Weeks, *J. Phys. Chem. B* **103**, 4570 (2005); D. Chandler, *Nature* **437**, 640 (2005).
- [22] S. Rajamani, T. M. Truskett, and S. Garde, *Proc. Natl. Acad. Sci. U.S.A.* **102**, 9475 (2005).
- [23] A. Frumkin, *Z. Phys. Chem.* **109**, 34 (1924).
- [24] S. L. Carnie and G. M. Torrie, *Adv. Chem. Phys.* **56**, 141 (1984).
- [25] D. Horinek and R. R. Netz, *Phys. Rev. Lett.* **99**, 226104 (2007).